Reversing Lindblad Dynamics via Continuous Petz Recovery Map

Hyukjoon Kwon,[1,2,*] Rick Mukherjee,[1] and M. S. Kim[1,2,†]

[1] *QOLS, Blackett Laboratory, Imperial College London, London SW7 2AZ, United Kingdom*
[2] *Korea Institute for Advanced Study, Seoul 02455, South Korea*

An important issue in developing quantum technology is that quantum states are so sensitive to noise. We propose a protocol that introduces reverse dynamics, in order to precisely control quantum systems against noise described by the Lindblad master equation. The reverse dynamics can be obtained by constructing the Petz recovery map in continuous time. By providing the exact form of the Hamiltonian and jump operators for the reverse dynamics, we explore the potential of utilizing the near-optimal recovery of the Petz map in controlling noisy quantum dynamics. While time-dependent dissipation engineering enables us to fully recover a single quantum trajectory, we also design a time-independent recovery protocol to protect encoded quantum information against decoherence. Our protocol can efficiently suppress only the noise part of dynamics thereby providing an effective unitary evolution of the quantum system.

The dynamics of an open quantum system is defined by the Hamiltonian of the system and its interaction with the environment. On tracing out the environment, the system undergoes a non-unitary evolution which can easily wash out coherence. For the realization of quantum technologies, it is crucial to protect the system from leaking quantum information due to its interaction with the environment. Considerable amount of efforts have been made to achieve this task through developing protocols to minimize added noise [1–4], finding noise-free zones [5–7], and correcting [8–17] or mitigating [18–20] errors. Especially in quantum error-correction (QEC), a universal recovery operation, the so-called Petz recovery map [21] has served as a useful mathematical tool to study the recovery of quantum information [12, 22–24] and state discrimination protocols [25, 26]. Based on the near-optimal recovery property of the map [12], approximate QEC [12, 14, 16] has been developed. However, due to its complexity, the Petz recovery map remains in the mathematical realm, while an approach to realize the discrete version of the map was proposed very recently [27].

In this Letter, we construct a quantum master equation which realizes the Petz recovery map in continuous time. While the Petz recovery map recovers a given quantum state after following noisy dynamics, a physical protocol to achieve the recovery map was not previously known. Our master equation identifies the reverse Hamiltonian and the jump operators that can fully reverse a quantum trajectory. We extend this to design a time-independent recovery protocol and use it to protect quantum information against decoherence. The efficient noise cancelation leads to a noiseless unitary dynamics of the encoded system. The recovery dynamics can be implemented by interacting the system with a strongly decaying ancilla.

Reversing quantum master equation dynamics.— We focus on a Markovian open quantum dynamics described by the Lindblad equation [28] ($\hbar = 1$):

$$\frac{d\rho}{dt} = \mathcal{L}(\rho) = -i[H,\rho] + \sum_{\mu} \mathcal{D}[L_\mu](\rho), \tag{1}$$

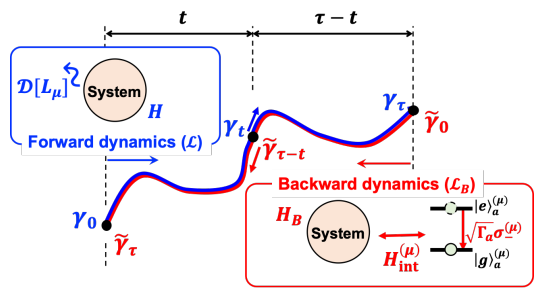

FIG. 1. Forward (reverse) dynamics $\mathcal{L}$ ($\mathcal{L}_B$) described by the Hamiltonian H (H_B) and jump operators L_μ ($L_{B,\mu}$). The reverse jump operators can be implemented by interaction Hamiltonian $H_{\text{int}}^{(\mu)}$ between the system and a strongly decaying ancilla state. See the main text for details.

where $\mathcal{D}[L_\mu](\rho) = L_\mu \rho L_\mu^\dagger - \frac{1}{2}\{L_\mu^\dagger L_\mu, \rho\}$. Here, $[A,B] = AB - BA$ and $\{A,B\} = AB + BA$. A quantum state γ_0 at time $t = 0$ then evolves to $\gamma_\tau = \mathcal{T}\left[\exp\left(\int_0^\tau \mathcal{L}dt\right)\right](\gamma_0)$ after some time $t = \tau$, where $\mathcal{T}$ is the time-ordering operator. We ask whether it is possible to recover the quantum state at each time from the final state γ_τ.

To reconstruct the initial state γ_0 from the final state γ_τ one can adopt the Petz recovery map [21], also known as the transpose channel. For a quantum channel $\mathcal{N}$ and a reference state ρ, the Petz recovery map defined as $\mathcal{R}_{\rho,\mathcal{N}}(\cdot) = \rho^{\frac{1}{2}}\mathcal{N}^\dagger(\mathcal{N}(\rho)^{-\frac{1}{2}}(\cdot)\mathcal{N}(\rho)^{-\frac{1}{2}})\rho^{\frac{1}{2}}$ recovers ρ from $\mathcal{N}(\rho)$, i.e.,

$$\mathcal{R}_{\rho,\mathcal{N}}(\mathcal{N}(\rho)) = \rho. \tag{2}$$

Such a property of the recovery map has been studied as a generalized time-reversal in various contexts, including quantum thermodynamics [29–31] and Bayesian retrodiction of quantum processes [32]. By taking a quantum channel $\mathcal{N} = \mathcal{T}\left[\exp\left(\int_0^\tau \mathcal{L}dt'\right)\right]$ as the forward dynamics after time τ and the reference state γ_0, the Petz recovery map recovers γ_0 from γ_τ, i.e., $\mathcal{R}_{\gamma_0,\mathcal{N}}(\gamma_\tau) = \gamma_0$.

Such a construction of the recovery map can be extended for any time $t \in [0,\tau]$, based on the dynamical semigroup property of the Lindblad equation. The Petz

recovery map in the limit of infinitesimal time interval can be described by the following Lindblad equation [31]:

$$\frac{d\rho}{d\tilde{t}} = \mathcal{L}_B(\rho) = -i[H_B(\tilde{t}), \rho] + \sum_\mu \mathcal{D}[L_{B,\mu}(\tilde{t})](\rho).$$

In this work, we show that the reverse dynamics can be expressed by the separate contributions of the forward Hamiltonian H and jump operators L_μ as

$$\begin{aligned} H_B(\tilde{t}) &= -H + \sum_\mu H_C(\gamma_{\tau-\tilde{t}}, L_\mu) \\ L_{B,\mu}(\tilde{t}) &= \gamma_{\tau-\tilde{t}}^{\frac{1}{2}} L_\mu^\dagger \gamma_{\tau-\tilde{t}}^{-\frac{1}{2}}, \end{aligned} \tag{3}$$

where the tilde indicates the backward direction and

$$H_C(\gamma, L_\mu) = -\frac{i}{2} \sum_{\lambda,\lambda'} \left(\frac{\sqrt{\lambda} - \sqrt{\lambda'}}{\sqrt{\lambda} + \sqrt{\lambda'}} \right) \langle\lambda| M_\mu(\gamma) |\lambda'\rangle |\lambda\rangle \langle\lambda'|,$$

using the eigenvalue decomposition $\gamma = \sum_\lambda \lambda |\lambda\rangle \langle\lambda|$ and defining $M_\mu(\gamma) = L_\mu^\dagger L_\mu + \gamma^{-\frac{1}{2}} L_\mu \gamma L_\mu^\dagger \gamma^{-\frac{1}{2}}$. If γ contains zero-eigenvalues, pseudo-inverse on its support can be taken [33] For a dissipation-free dynamics, the reverse dynamics takes the form $\mathcal{L}_B(\rho) = -i[H_B, \rho]$ with $H_B = -H$, while $L_{B,\mu}$ and H_C contribute to reversing the dissipation $\mathcal{D}[L_\mu]$. The reverse dynamics fully recovers the quantum trajectory (see Fig. 1), i.e.,

$$\tilde{\gamma}_{\tilde{t}=\tau-t} = \mathcal{T}\left[e^{\int_0^{\tau-t} \mathcal{L}_B d\tilde{t}'} \right] (\gamma_\tau) = \gamma_t, \quad \forall t \in [0, \tau], \tag{4}$$

as it satisfies $\mathcal{L}_B(\tilde{\gamma}_{\tilde{t}=\tau-t}) = -\mathcal{L}(\gamma_t)$. We note that the forward trajectory information γ_t is required to construct the reverse dynamics. This can, in principle, be calculated from the initial state γ_0 and the forward dynamics $\mathcal{L}$, without performing state tomography. The explicit form of the reverse dynamics in Eq. (3) brings the abstract mathematical expression of the Petz recovery map into a physically achievable form, by identifying the Hamiltonian and jump operators.

As an illustrative example, we consider a two-level system whose dynamics is given by a Hamiltonian $H = \boldsymbol{h} \cdot \boldsymbol{\sigma}$ and a single jump operator $L = \boldsymbol{l} \cdot \boldsymbol{\sigma}$, where $\boldsymbol{\sigma} = (\sigma_x, \sigma_y, \sigma_z)$ are the Pauli operators, and $\boldsymbol{h}$ and $\boldsymbol{l}$ are real and complex vectors, respectively. Figure 2 shows that the reverse dynamics with $H_B = \boldsymbol{h}_B \cdot \boldsymbol{\sigma}$ and $L_B = \boldsymbol{l}_B \cdot \boldsymbol{\sigma}$ obtained from Eq. (3) fully reverses the quantum trajectory for the reference state $|0\rangle$ such that $\sigma_z |0\rangle = |0\rangle$. This requires a temporal control of $\boldsymbol{h}_B$ and $\boldsymbol{l}_B$ with three and six independent parameters, respectively, where their closed forms and the implicit implementation of the jump operator can be found in the Supplemental Material [33].

Continuous-time recovery with time-independent control.— To avoid the temporal control of multiple parameters which can be technically challenging, we extend the recovery protocol to have *time-independent* Hamiltonian and jump operators. To this end, we

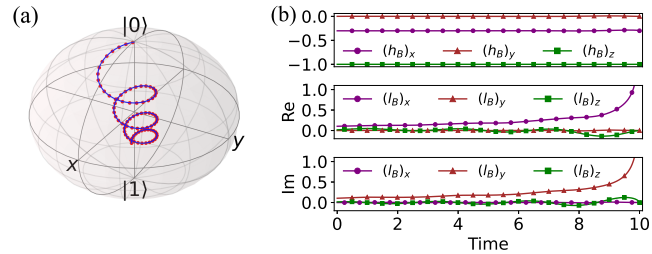

FIG. 2. (a) The forward (solid) and backward (dotted) trajectories of the qubit dynamics of $H = 0.3\sigma_x + \sigma_z$, and $L = 0.4\sigma_-$ with $\tau = 10$ and $\gamma_0 = |0\rangle\langle 0|$. (b) The Hamiltonian and jump operators for the reverse dynamics.

consider the scenario where the forward and recovery dynamics simultaneously act on the system as,

$$\mathcal{L}_S(\rho) = (\mathcal{L} + \mathcal{L}_B)(\rho) = \mathcal{L}(\rho) - i[H_B, \rho] + \sum_\mu \mathcal{D}[L_{B,\mu}](\rho), \tag{5}$$

where $H_B = -H + \sum_\mu H_C(\gamma, L_\mu)$ and $L_{B,\mu} = \gamma^{\frac{1}{2}} L_\mu^\dagger \gamma^{-\frac{1}{2}}$ for a full-rank reference state γ. We note that γ becomes a stationary state satisfying $\dot{\gamma} = \mathcal{L}_S(\gamma) = 0$. This can be understood as the infinitesimal time recovery $\mathcal{L}_B$ cancels out the effect of noise $\mathcal{L}$, hence trapping a fixed reference state γ instead of reversing a trajectory γ_t. As being less resource intensive in its implementation, henceforth, we focus on the time-independent formalism described by Eq. (5) for the applications of our recovery protocol.

Recovery of encoded quantum information.— While the Petz recovery map perfectly recovers the reference state, the map also enjoys the universal recovery property such that a wider spectrum of quantum states encoded in a higher-dimensional Hilbert space can be recovered close to the optimal rate [12]. In this manner, our continuous-time recovery protocol not only keeps the full-rank reference state static but also well protects any encoded quantum states, regardless of their ranks. This can be demonstrated by constructing the code space $\mathcal{C}$ spanned by the degenerate ground states of a Hermitian operator Q and applying the reverse dynamics in Eq. (5) with the following form of the reference state:

$$\gamma = \frac{e^{-\beta Q}}{\mathrm{Tr}\left[e^{-\beta Q}\right]}. \tag{6}$$

This form guarantees that γ is full-ranked and becomes proportional to the projector onto the code space $P_\mathcal{C} = \sum_{|\psi\rangle \in \mathcal{C}} |\psi\rangle\langle\psi|$ when $\beta \gg 1$, which was shown to be the reference state that efficiently preserves the code space's information [37].

As an example, we consider a fully-connected n-spin chain with $Q = -\sum_{i>j} \sigma_z^{(i)} \sigma_z^{(j)}$, where $\sigma_{x,y,z}^{(i)}$ acts on the ith spin. A logical qubit is then spanned by the degenerate ground states of Q as $|\psi\rangle = \alpha_0 |0\rangle^{\otimes n} +$

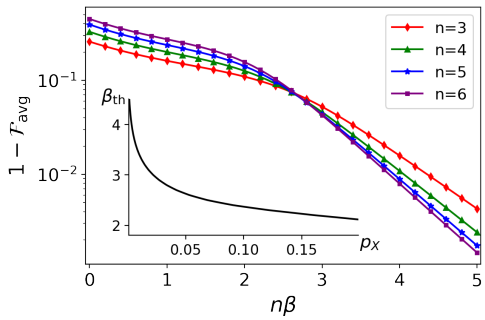

FIG. 3. The average infidelity $1-\mathcal{F}_{\rm avg}$ (main plot) and threshold value $\beta_{\rm th}$ (inset) of a single logical qubit after applying the recovery. For the main plot, the bit-flipping probability of each physical qubit is taken to be $p_X = 0.05$.

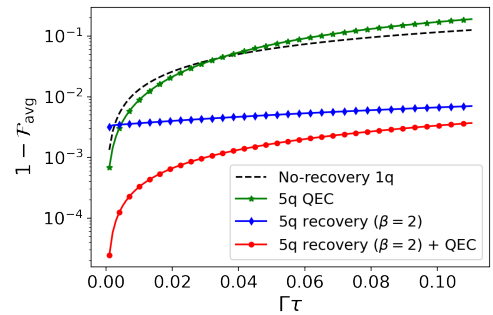

FIG. 4. Comparison between the average infidelities of the $[\![5,1,3]\!]$ code by applying the continuous recovery protocol and QEC. The noise is given with $\Gamma_X = \Gamma_Z = \Gamma$ and $\Gamma_{ZZ} = 0.2\Gamma$ and the time is given in a unit of $1/\Gamma$.

$\alpha_1 |1\rangle^{\otimes n} \in \mathcal{C}$. We show that the logical qubit can be efficiently protected against the noise dynamics $\mathcal{L}_X = \Gamma_X \sum_{i=1}^n \mathcal{D}[\sigma_x^{(i)}]$, which is equivalent to independent bit-flipping errors on each qubit with probability $p_X = (1-e^{-2\Gamma_X\tau})/2$ after time τ. The recovery dynamics of Eq. (5) is constructed by noting that $\gamma^{\frac{1}{2}}\sigma_x^{(i)}\gamma^{-\frac{1}{2}} = \sigma_x^{(i)}\prod_{j\neq i}\left[(\cosh\beta)\mathbb{1} - (\sinh\beta)\sigma_z^{(i)}\sigma_z^{(j)}\right]$ and $H_C(\gamma, \sigma_x^{(i)}) = 0$. Figure 3 shows that the average fidelity $\mathcal{F}_{\rm avg} = \int_{|\psi\rangle\in\mathcal{C}} d\psi \langle\psi| e^{\mathcal{L}_S\tau}(|\psi\rangle\langle\psi|)|\psi\rangle$ increases as β becomes larger. To obtain a larger value of β, stronger recovery is required, which can be captured by $\cosh\beta$ and $\sinh\beta$ terms in the jump operators. We also note that increasing the number of physical qubits n provides a higher recovery rate when $n\beta$ exceeds a threshold $\beta_{\rm th}$. We observe that $\beta_{\rm th}$ becomes smaller when the bit-flipping rate p_X increases (see Fig. 3), implying that a weak recovery dynamics can be effective for an intermediate noise level.

Continuous recovery protocol for QEC codes.— The code space of the fully-connected spin can be understood using the stabilizer formalism in QEC. We further provide a general expression of the recovery protocol for any $[\![n,k,d]\!]$ stabilizer code, which encodes k-logical qubits into n-physical qubits with code distance d. Such a code construction is efficient for the Pauli-type dissipation $\mathcal{L} = \sum_\mu \Gamma_\mu \mathcal{D}[E_\mu]$ with $E_\mu \in \langle\sigma_x,\sigma_y,\sigma_z\rangle^n$. The code space $\mathcal{C}$ is spanned by a set of quantum states that commute with every element in a stabilizer $\mathcal{S}$. By noting that every state in $\mathcal{C}$ becomes a ground state of $Q = -\sum_{S_i\in\bar{\mathcal{S}}} S_i$ for a subset of the stabilizer $\bar{\mathcal{S}} \subset \mathcal{S}$, often referred to as the stabilizer Hamiltonian, the recovery dynamics becomes

$$\mathcal{L}_B = \sum_\mu \Gamma_\mu \mathcal{D}\left[E_\mu \prod_{S_i\in\bar{\mathcal{S}}_\mu} [(\cosh\beta)\mathbb{1} - (\sinh\beta)S_i]\right], \quad (7)$$

where $\bar{\mathcal{S}}_\mu = \{S_i \in \bar{\mathcal{S}} | \{S_i, E_\mu\} = 0\}$. For $\beta \gg 1$ and E_μ in the correctable set, Eq. (7) can be interpreted as continuous syndrome measurements and corrections, which have been studied in the context of continuous QEC [38–41] and experimentally realized in circuit QED [42–44].

For example, we consider a noise model $\mathcal{L} = \sum_{i=1}^5 \left(\Gamma_X\mathcal{D}[\sigma_x^{(i)}] + \Gamma_Z\mathcal{D}[\sigma_Z^{(i)}] + \Gamma_{ZZ}\mathcal{D}[\sigma_z^{(i)}\sigma_z^{(i+1)}]\right)$ and its recovery protocol applied to the $[\![5,1,3]\!]$ code [9, 10] by taking $Q = -\sum_{i=1}^5 \sigma_x^{(i)}\sigma_z^{(i+1)}\sigma_z^{(i+2)}\sigma_x^{(i+3)}$, where $\sigma_{x,z}^{(5l+j)} = \sigma_{x,z}^{(j)}$ for $l \in \mathbb{Z}$. Figure 4 shows that the noise is suppressed by applying the recovery protocol, even for the correlated noise which cannot be directly handled with the $[\![5,1,3]\!]$ code. We also note that conventional syndrome-measurement-based QEC becomes more effective after suppressing noise via the continuous recovery protocol. For $\Gamma_X = \Gamma_Z = \Gamma$ and $\Gamma_{ZZ} = 0.2\Gamma$, QEC is effective for all the time when the recovery is active. In contrast, without the recovery protocol, QEC is effective only for $\Gamma\tau \lesssim 0.03$ (see Fig. 4). This shows that the continuous recovery can aid QEC by reducing the noise level below the threshold, as it can be applied to more complicated stabilizer codes [13, 15].

Meanwhile, our approach is not limited to the stabilizer code or Pauli-type dissipation. From any code space $\mathcal{C}$, one can take $Q = -P_\mathcal{C}$ to construct the recovery protocol. In the limit of $\beta \gg 1$, we obtain $\mathcal{L}_B \approx e^\beta \sum_\mu \mathcal{D}[P_\mathcal{C} L_\mu^\dagger (\mathbb{1} - P_\mathcal{C})]$, which can be understood as a continuous-time quantum jump from outside of the code space $(\mathbb{1} - P_\mathcal{C})$ to the code space $(P_\mathcal{C})$. Such a construction is useful to achieve efficient protection of quantum states by noise-specific encoding. Other noise models, including amplitude damping, with various types of the code space construction are discussed in the Supplemental Material [33].

For the both recovery protocols based on stabilizer and general code spaces, the reference state γ does not need to be prepared to implement the recovery dynamics as it can be fully determined only from Q and β. The average error is governed by the factor β, which can be interpreted as the inverse temperature by noting that the most states remain at the ground state, i.e., the code space at the

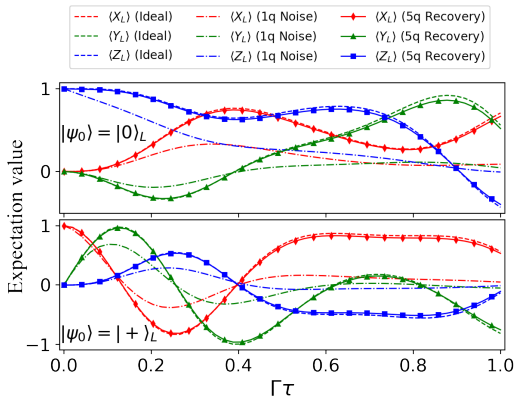

FIG. 5. Simulating the dynamics of the $[\![5,1,3]\!]$ code under a time-dependent Hamiltonian $H_L(t) = 3\sin(5t)X_L + 6\cos(2t)Z_L$. The initial states are prepared in $|0\rangle_L$ (top) and $|+\rangle_L = (|0\rangle_L + |1\rangle_L)/\sqrt{2}$ (bottom), respectively, and the same recovery operation $\mathcal{L}_B$ with $\beta = 2$ is applied to the both cases without QEC. The noise model is the same as in Fig. 4.

low temperature ($\beta \gg 1$). In this limit, the code space $\mathcal{C}$ becomes a decoherence-free subspace of the reverse dynamics $\mathcal{L}_B$, and at the same time, $\mathcal{L}_B$ continuously brings quantum states outside the code space back to the code space. From the similarity appearing in the stationary state in Eq. (6), the recovery map can be compared to self-correcting quantum memory [45–47]. However, we highlight that our recovery dynamics in Eq. (5) meets the quantum detailed balance relation [48] even without the Davies map condition [49].

The recovery protocol not only provides a longer lifetime of logical qubits, but also can be utilized to simulate noise-free dynamics of a logical Hamiltonian $H_L(t)$ acting on the code space. In the following dynamics,

$$\dot{\rho} = -i[H_L(t), \rho] + \mathcal{L}(\rho) + \mathcal{L}_B(\rho), \tag{8}$$

the recovery $\mathcal{L}_B$ continuously cancels out the noise $\mathcal{L}$, thereby a quantum state $\rho_{\mathcal{C}}$ in the code space evolves effectively unitarily, $\dot{\rho}_{\mathcal{C}} \approx -i[H_L(t), \rho_{\mathcal{C}}]$. Figure 5 shows the effective unitary dynamics of the $[\![5,1,3]\!]$ code under Eq. (8), where the logical operations are defined as $X_L = \bigotimes_{i=1}^{5} \sigma_x^{(i)}$ and $Z_L = \bigotimes_{i=1}^{5} \sigma_z^{(i)}$. We note that the same recovery protocol is applied to any initial states in the code space.

Implementation of the reverse dynamics and resource analysis.— The dissipation engineering for the continuous recovery map can be done by introducing a strongly-decaying ancillary system. Assuming a two-level ancilla state, the jump operators $L_{B,\mu}$ can be implemented throughout the system-ancilla interaction,

$$H_{\text{int}}^{(\mu)} = \frac{1}{2}\left(L_{B,\mu}^{\dagger} \otimes \sigma_-^{(\mu)} + L_{B,\mu} \otimes \sigma_+^{(\mu)}\right), \tag{9}$$

and the dissipation of the ancilla $\Gamma_a \mathcal{D}[\sigma_-^{(\mu)}]$. In the limit of strong dissipation, one can adiabatically eliminate the excited states of the ancilla so that the system's effective dynamics can be well approximated as $(1/\Gamma_a)\mathcal{D}[L_{B,\mu}]$ [50]. Thus, by tuning the Hamiltonian of the total system to be $H_{sa} = H_B + \sqrt{\Gamma_a}\sum_\mu H_{\text{int}}^{(\mu)}$, the dynamics

$$\mathcal{L}_{sa}(\rho_{sa}) = -i[H_{sa}, \rho_{sa}] + \Gamma_a \sum_\mu \mathcal{D}[\sigma_-^{(\mu)}](\rho_{sa}), \tag{10}$$

leads to the effective system dynamics $\mathcal{L}_B$ after tracing out the ancilla system. The strength of the engineered dissipation can be expressed in terms of a dimensionless parameter $\|H_{sa}\|^2/(\Gamma_a\Gamma_\mu)$ [41], where $\Gamma_\mu = \|L_\mu\|^2$ is the intrinsic dissipation strength of the system. In order to engineer the dissipation successfully, we need to satisfy $\Gamma_a \gg \|H_{sa}\| \gg \sqrt{\Gamma_a\Gamma_\mu}$. This condition can be achieved in ultracold and circuit QED systems. In particular with Rydberg systems, both the strength of the system-ancilla interaction and the decay rate of an effective two-level system can be controlled either by choosing a specific principal quantum number or by applying the concept of Rydberg dressing [51, 52]. This flexibility can provide a whole range of values for $\|H_{sa}\| \sim$ MHz to GHz while $\Gamma_a, \Gamma_\mu \sim$ kHz to tens MHz [53].

For the qubit system considered in Fig. 2, $H_{\text{int}}^{(\mu)}$ requires two-qubit Pauli operations between the system and ancilla. One way to construct a Hamiltonian with universal two-body interactions would be to use superconducting qubits [54]. Another possible route would be to use ultracold systems. Examples of engineering general two-body spin interactions involve cold atoms [55], ions [56], and anisotropic interactions between Rydberg atoms [57] or polar molecules [58]. On the other hand, characterizing the noise and engineering of jump operators of a multi-qubit system might be a challenging task to achieve the continuous recovery protocol. Nevertheless, recent progress on dissipation engineering [50, 59–61] could lead to resolving technical challenges.

The total number of qubits required to achieve the reverse dynamics for n-physical qubits is $n + n_a$, where n_a is the number of ancilla qubits to implement the reverse jump operators. We note that n_a equals the number of jump operators describing noise acting on n-physical qubits, no matter local or correlated. For a local noise model, n_a linearly scales with n, which is comparable to the number of ancilla qubits required for syndrome measurements in the standard QEC. When noise at each physical qubit has pairwise correlations with at most ℓ other qubits, n_a scales no more than $\mathcal{O}(n\ell)$. In addition, the time-independent recovery protocol takes the advantage that it does not require system controls conditioned on the syndrome measurement outcomes, as well as additional classical computation for diagnosing the errors from the syndromes.

Remarks.— We have shown that Lindblad dynamics can be reversed by constructing the Petz recovery map in continuous time. We have provided an explicit form of

the Hamiltonian and jump operators as well as a possible route for physical realization of such dynamics throughout the adiabatic elimination technique. As an application, we have shown that the continuous recovery protocol can be designed for QEC, which provides a high recovery rate of encoded quantum information against noisy environment.

Our recovery protocol can be applied to implementing a noiseless quantum gate [62, 63] and dynamical quantum noise cancelling [64], which might be feasible for small scale noisy quantum devices [65]. This will open a new possibility to utilize the near-optimal recovery property of the Petz recovery map not only in approximate QEC [12, 14, 16] and quantum communication [66], but also revealing fundamental physics in quantum thermodynamics [29–31] and the AdS/CFT correspondence [67, 68]. Our formalism is limited to Markovian noise but can be further generalized to a noise model with time-dependent jump operators. An interesting future research would be exploring whether this formalism can be extended to non-Markovian dynamics, such as $1/f$ noise in superconducting qubits [69, 70].

This work is supported by the KIST Open Research Program, the QuantERA ERA-NET within the EU Horizon 2020 Programme and the UK Hub in Quantum Computing and Simulation, part of the UK National Quantum Technologies Programme with funding from UKRI EPSRC grants EP/T001062/1 and EP/R044082/1. MSK acknowledges the KIAS visiting professorship.

* hjkwon@kias.re.kr
† m.kim@imperial.ac.uk

[1] M. D. LaHaye, O. Buu, B. Camarota, K. C. Schwab, *Approaching the Quantum Limit of a Nanomechanical Resonator*, Science **304**, 74 (2004).

[2] I. Wilson-Rae, P. Zoller, and A. Imamoğlu, *Laser Cooling of a Nanomechanical Resonator Mode to its Quantum Ground State*, Phys. Rev. Lett. **92**, 075507 (2004).

[3] S. Gigan, H. R. Böhm, M. Paternostro, F. Blaser, G. Langer, J. B. Hertzberg, K. C. Schwab, D. Bäuerle, M. Aspelmeyer, and A. Zeilinger, *Self-cooling of a micromirror by radiation pressure*, Nature **444**, 67 (2006).

[4] D. E. Chang, C. A. Regal, S. B. Papp, D. J. Wilson, J. Ye, O. Painter, H. J. Kimble, and P. Zoller, *Cavity optomechanics using an optically levitated nanosphere* Proc. Natl. Acad. Sci. USA **107**, 1005 (2010).

[5] D. A. Lidar, I. L. Chuang, and K. B. Whaley, *Decoherence-Free Subspaces for Quantum Computation*, Phys. Rev. Lett. **81**, 2594 (1998).

[6] L. Viola, E. Knill, and S. Lloyd, *Dynamical Decoupling of Open Quantum Systems*, Phys. Rev. Lett. **82**, 2417 (1999).

[7] P. Facchi, D. A. Lidar, and S. Pascazio, *Unification of dynamical decoupling and the quantum Zeno effect*, Phys. Rev. A **69**, 032314 (2004).

[8] P. W. Shor, *Scheme for reducing decoherence in quantum computer memory*, Phys. Rev. A **52**, 2493(R) (1995).

[9] C. H. Bennett, D. P. DiVincenzo, J. A. Smolin, and W. K. Wootters, *Mixed-state entanglement and quantum error correction*, Phys. Rev. A **54**, 3824 (1996).

[10] R. Laflamme, C. Miquel, J. P. Paz, and W. H. Zurek, *Perfect Quantum Error Correcting Code*, Phys. Rev. Lett. **77**, 198 (1996).

[11] D. Gottesman, *Stabilizer Codes and Quantum Error Correction*, PhD thesis (CalTech, Pasadena, 1997).

[12] H. Barnum and E. Knill, *Reversing quantum dynamics with near-optimal quantum and classical fidelity*, J. Math. Phys. **43**, 2097 (2002).

[13] A. Kitaev, *Anyons in an Exactly Solved Model and Beyond*, Ann. Phys. **321**, 2 (2006).

[14] H. K. Ng and P. Mandayam, *Simple approach to approximate quantum error correction based on the transpose channel*, Phys. Rev. A **81**, 062342 (2010).

[15] A. G. Fowler, M. Mariantoni, J. M. Martinis, and A. N. Cleland, *Surface codes: Towards practical large-scale quantum computation*, Phys. Rev. A **86**, 032324 (2012).

[16] C. Cafaro and P. van Loock, *Approximate quantum error correction for generalized amplitude-damping errors*, Phys. Rev. A **89**, 022316 (2014).

[17] M. A. Nielsen and I. L. Chuang, *Quantum Computation and Quantum Information*, Cambridge Series on Information and the Natural Sciences (Cambridge University Press, Cambridge, 2000).

[18] K. Temme, S. Bravyi, and J. M. Gambetta, *Error Mitigation for Short-Depth Quantum Circuits*, Phys. Rev. Lett. **119**, 180509 (2017).

[19] Y. Li and S. C. Benjamin, *Efficient Variational Quantum Simulator Incorporating Active Error Minimization*, Phys. Rev. X **7**, 021050 (2017).

[20] S. Endo, S. C. Benjamin, and Y. Li, *Practical Quantum Error Mitigation for Near-Future Applications*, Phys. Rev. X **8**, 031027 (2018).

[21] D. Petz, *Sufficient Subalgebras and the Relative Entropy of States of a von Neumann Algebra*, Commun. Math. Phys.**105**, 123 (1986).

[22] M. M. Wilde, *Recoverability in Quantum Information*, Theory, Proc. R. Soc. A **471**, 20150338 (2015).

[23] D. Sutter, M. Tomamichel, and A. W. Harrow, *Strengthened Monotonicity of Relative Entropy via Pinched Petz Recovery Map*, IEEE Trans. Inf. Theory **62**, 2907 (2016).

[24] M. Junge, R. Renner, D. Sutter, M. M. Wilde, and A. Winter, *Universal Recovery Maps and Approximate Sufficiency of Quantum Relative Entropy*, Ann. Inst. Henri Poincaré **19**, 2955 (2018).

[25] A. S. Holevo, *On asymptotically optimal hypothesis testing in quantum statistics*, Theory Probab. Appl. **23**, 411 (1979).

[26] P. Hausladen and W. K. Wootters, *A 'pretty good' measurement for distinguishing quantum states*, J. Mod. Optics **41**, 2385 (1994).

[27] A. Gilyén, S. Lloyd, I. Marvian, Y. Quek, and M. M. Wilde, *Quantum algorithm for Petz recovery channels and pretty good measurements*, arXiv:2006.16924.

[28] G. Lindblad, *On the generators of quantum dynamical semigroups*, Commun. Math. Phys. **48**, 119 (1976).

[29] P. Faist and R. Renner, *Fundamental Work Cost of Quantum Processes*, Phys. Rev. X **8**, 021011 (2018).

[30] J. Åberg, *Fully Quantum Fluctuation Theorems*, Phys. Rev. X **8**, 011019 (2018).

[31] H. Kwon and M. S. Kim, *Fluctuation Theorems for a Quantum Channel*, Phys. Rev. X **9**, 031029 (2019).

[32] F. Buscemi and V. Scarani, *Fluctuation theorems from Bayesian retrodiction*, Phys. Rev. E **103**, 052111(2021).

[33] See Supplemental Material and references [34–36] within it for the proofs and detailed analysis.

[34] M. Horodecki, P. Horodecki, and R. Horodecki, *General teleportation channel, singlet fraction, and quasidistillation*, Phys. Rev. A **60**, 1888 (1999).

[35] M. A. Nielsen, *A simple formula for the average gate fidelity of a quantumdynamical operation*, Phy. Lett. A **303** 249 (2002).

[36] M. Zwolak and G. Vidal, *Mixed-State Dynamics in One-Dimensional Quantum Lattice Systems: A Time-Dependent Superoperator Renormalization Algorithm*, Phys. Rev. Lett. **93**, 207205 (2004).

[37] R. Blume-Kohout, H. K. Ng, D. Poulin, and L. Viola, Phys. Rev. Lett. **100**, 030501 (2008).

[38] J. P. Paz and W. H. Zurek, *Continuous error correction*, Proc. R. Soc. A **454**, 355 (1998).

[39] M. Sarovar and G. J. Milburn, *Continuous quantum error correction by cooling*, Phys. Rev. A **72**, 012306 (2005)

[40] F. Pastawski, L. Clemente, and J. I. Cirac, *Quantum memories based on engineered dissipation*, Phys. Rev. A **83**, 012304 (2011).

[41] J.-M. Lihm, K. Noh, and U. R. Fischer, *Implementation-independent sufficient condition of the Knill-Laflamme type for the autonomous protection of logical qudits by strong engineered dissipation*, Phys. Rev. A **98**, 012317 (2018).

[42] Z. Leghtas, S. Touzard, I. M. Pop, A. Kou, B. Vlastakis, A. Petrenko, K. M. Sliwa, A. Narla, S. Shankar, M. J. Hatridge, M. Reagor, L. Frunzio, R. J. Schoelkopf, M. Mirrahimi, and M. H. Devoret, *Confining the state of light to a quantum manifold by engineered two-photon loss*, Science **347**, 853 (2015).

[43] S. Touzard, A. Grimm, Z. Leghtas, S. O. Mundhada, P. Reinhold, C. Axline, M. Reagor, K. Chou, J. Blumoff, K. M. Sliwa, S. Shankar, L. Frunzio, R. J. Schoelkopf, M. Mirrahimi, and M. H. Devoret, *Coherent Oscillations Inside a Quantum Manifold Stabilized by Dissipation*, Phys. Rev. X **8**, 021005 (2018).

[44] J. M. Gertler, B. Baker, J. Li, S. Shirol, J. Koch, and C. Wang, *Protecting a bosonic qubit with autonomous quantum error correction*, Nature, **590**, 243 (2021).

[45] E. Dennis, A. Kitaev, A. Landahl, and J. Preskill, *Topological quantum memory*, J. Math. Phys. (N.Y.) **43**, 4452 (2002).

[46] R. Alicki, M. Horodecki, P. Horodecki, and R. Horodecki, *On Thermal Stability of Topological Qubit in Kitaev's 4D Model*, Open Syst. Inf. Dyn. **17**, 1 (2010).

[47] S. Bravyi and J. Haah, *Quantum Self-Correction in the 3D Cubic Code Model*, Phys. Rev. Lett. **111**, 200501 (2013).

[48] Á. M. Alhambra and M. P. Woods, *Dynamical maps, quantum detailed balance, and the Petz recovery map*, Phys. Rev. A **96**, 022118 (2017).

[49] E. Davies, *Markovian master equations*, Commun. Math. Phys. **39**, 91 (1974).

[50] F. Verstraete, M. M. Wolf, and J. I. Cirac, *Quantum computation and quantum-state engineering driven by dissipation*, Nature Phys. **5**, 633 (2009).

[51] R. Mukherjee, T. C. Killian, and K. R. A. Hazzard, *Accessing Rydberg-dressed interactions using many-body Ramsey dynamics*, Phys. Rev. A **94**, 053422 (2016).

[52] J. Zeiher, R. van Bijnen, P. Schauß, S. Hild, J.-y. Choi, T. Pohl, I. Bloch, and C. Gross, *Many-body interferometry of a Rydberg-dressed spin lattice*, Nat. Phys. **12**, 1095 (2016).

[53] M. Saffman, T. G. Walker, and K. Mølmer, *Quantum information with Rydberg atoms*, Rev. Mod. Phys. **82**, 2313 (2010).

[54] E. Kapit, *Universal two-qubit interactions, measurement, and cooling for quantum simulation and computing*, Phys. Rev. A **92**, 012302 (2015).

[55] C.-L. Hung, A. González-Tudela, J. I. Cirac, and H. J. Kimble, *Quantum spin dynamics with pairwise-tunable, long-range interactions*, Proc. Nat. Academy of Sciences **113**, E4946 (2016).

[56] K. Kim, M. S. Chang, S. Korenblit, R. Islam, E. E. Edwards, J. K. Freericks, G. D. Lin, L. M. Duan, and C. Monroe, *Quantum simulation of frustrated Ising spins with trapped ions*, Nature **465**, 590 (2010).

[57] A. W. Glaetzle, M. Dalmonte, R. Nath, C. Gross, I. Bloch, and P. Zoller, *Designing Frustrated Quantum Magnets with Laser-Dressed Rydberg Atoms*, Phys. Rev. Lett. **114**, 173002 (2015).

[58] M. L. Wall, K. R. A. Hazzard, and A. M. Rey, *Quantum magnetism with ultracold molecules*, *From Atomic to Mesoscale*, Chap. 1, pp. 3-37.

[59] G. Morigi, J. Eschner, C. Cormick, Y. Lin, D. Leibfried, and D. J. Wineland, *Dissipative Quantum Control of a Spin Chain*, Phys. Rev. Lett. **115**, 200502 (2015).

[60] K. P. Horn, F. Reiter, Y. Lin, D. Leibfried, and C. P. Koch, *Quantum optimal control of the dissipative production of a maximally entangled state*, New J. Phys. **20**, 123010 (2018).

[61] F. Damanet, E. Mascarenhas, D. Pekker, and A. J. Daley *Controlling Quantum Transport via Dissipation Engineering*, Phys. Rev. Lett. **123**, 180402 (2019).

[62] J. Sun, X. Yuan, T. Tsunoda, V. Vedral, S. C. Benjamin, and S. Endo, *Mitigating realistic noise in practical noisy intermediate-scale quantum devices*, arXiv:2001.04891.

[63] J. W. Z. Lau, K. Bharti, T. Haug, and L. C. Kwek, *Quantum assisted simulation of time dependent Hamiltonians*, arXiv:2101.07677.

[64] M. Tsang and C. M. Caves, *Coherent Quantum-Noise Cancellation for Optomechanical Sensors*, Phys. Rev. Lett. **105**, 123601 (2010).

[65] J Preskill, *Quantum Computing in the NISQ era and beyond*, Quantum **2**, 79 (2018).

[66] S. Beigi, N. Datta, and F. Leditzky, *Decoding quantum information via the Petz recovery map*, J. Math. Phys. **57**, 082203 (2016).

[67] J. Cotler, P. Hayden, G. Penington, G. Salton, B. Swingle, and M. Walter, *Entanglement Wedge Reconstruction via Universal Recovery Channels*, Phys. Rev. X **9**, 031011 (2019).

[68] H. F. Jia and M. Rangamani, *Petz Reconstruction in Random Tensor Networks*, arXiv:2006.12601.

[69] R. W. Simmonds, K. M. Lang, D. A. Hite, S. Nam, D. P. Pappas, and J. M. Martinis, *Decoherence in Josephson Phase Qubits from Junction Resonators*, Phys. Rev. Lett. **93**, 077003 (2004).

[70] R. H. Koch, D. P. DiVincenzo, and J. Clarke, *Model for $1/f$ Flux Noise in SQUIDs and Qubits*, Phys. Rev. Lett. **98**, 267003 (2007).